Molecular Dynamics of DNA Origami Nanostructures

Annual Report for
Blue Waters Allocation

Aleksei Aksimentiev – Principal Investigator

January 31, 2016

Center for the Physics of Living Cells
Department of Physics
University of Illinois at Urbana-Champaign

Executive summary

DNA origami is a rapidly emerging technology that enables high-throughput construction of DNA-based sub-micron-size nanomachines with nanoscale accuracy. Similar to the computer-aided design (CAD) of macroscopic machines (e.g., airplanes), our group is pioneering CAD for nanoscale machines made of DNA origami. To achieve accuracy high enough to predict both chemical and mechanical properties of DNA origami objects, we employ all-atom molecular dynamics (MD) simulations. The Blue Waters supercomputer is essential for achieving this goal due to the sheer size of the DNA origami objects and computationally demanding nature of the MD technique. In this report, we present our achievements using the JQ5 allocation for the year of 2015, including a characterization of a prototypical DNA-based channel, a landmark simulation of a sub-micron DNA sculpture, and a comparative study of emerging DNA nanotechnologies. We request 240,000 node hours for 2016 to expand the design space of biomimetic ion channels and determine the physical mechanism underlying regulation of the shape-base assembly of DNA nanostructures.

Description of research activities and results

Key challenges

Self-assembly of DNA into complex three-dimensional objects has emerged as a new paradigm for practical nanotechnology [1, 2]. Among the methods that have been put forward that utilize self-assembly of DNA [2], DNA origami [3] stands out due to its conceptual simplicity and infinite range of possible applications [1, 2]. The basic principle of DNA origami is the programmed folding of a long (thousands of nucleotides) DNA strand into a custom two- or three-dimensional (3D) shape, guided by specially designed short oligonucleotides [3]. Since its first demonstration in 2006, the DNA origami method has advanced to encompass self-assembly of complex 3D objects with sub-nanometer precision [4] including static structures [1, 2, 5, 6] as well as objects that perform active functions [7, 8, 9]. Recent methodological advances [10] have made practical applications [10, 11, 12, 13] of DNA origami feasible.

Experimental characterization of DNA origami is essential for accurate design, but has been limited to rather qualitative techniques such as atomic force spectroscopy [7], small-angle X-ray scattering [7], and transmission electron microscopy (TEM) [4, 5]. Recently, super-resolution optical imaging [9], fluorescence resonance energy transfer (FRET) [12, 14] and magnetic tweezers [15] have been applied to DNA origami objects to infer information about their *in situ* structure and dynamics. The only atomic-level model of DNA origami *in situ* has been derived from cryo-electron microscopy (cryo-EM) [16], which revealed considerable deviations from the idealized design. Here, we describe our ongoing efforts to develop a computational approach that can replace the experimental characterization procedure to facilitate novel DNA origami designs that function as desired.

Why it Matters

Predictive computational modeling of DNA origami objects is an attractive alternative to experimental characterization procedures, which are expensive and time-consuming. It is already common practice for experimentalists to use the simplest available computational description of DNA—a continuum-based model—to validate their designs [17, 18]. In these models, DNA double helices are approximated as uniform cylinders with material properties set to reproduce the average bending rigidity of DNA helices. Unfortunately, this level of description permits only semi-quantitative estimation of the overall structure [18]. There are also several coarse-grained models of DNA that are more sophisticated than continuum-based models and can represent the double-helical structure of DNA [19, 20, 21]. In a typical coarse-grained DNA model, each nucleotide is represented by 2–3 interaction beads. When the interaction parameters are properly optimized, such models have the potential to make realistic predictions. However, these models are new and their accuracy is not well-established.

Currently, the most accurate computational method that can realize our goal—prediction of structure and function of DNA origami objects—is the all-atom molecular dynamics (MD) method. In 2013, we reported the first MD simulations of several model DNA origami systems [22]. Our simulation results were in exceptional agreement with the experimentally determined structural characteristics, proving the unmatched accuracy of the MD approach.

Since then, we have been trailblazing the application of the MD method to DNA origami objects by investigating various real-world problems. Our recent work includes a study of a DNA-based channel embedded in a lipid bilayer, a landmark simulation of a DNA sculpture that demonstrates the predictive power of the MD method for structure determination, and a detailed comparison between DNA origami and an emerging nanotechnology known as DNA bricks. The current status of these projects is summarized in the Accomplishments section. These studies, along with future investigations, will facilitate the ongoing development of MD-simulation protocols for predictive modeling of DNA origami objects. Moreover, we will continue to demonstrate the utility of the MD simulation technique to design novel DNA origami systems.

Why Blue Waters

DNA origami nanostructures can be as large as 30 nm on each side [7, 11, 16]. Although rough estimation of their structures can be done using simpler models [17], accurate prediction of structure requires an all-atom approach [22]. Furthermore, all-atom MD simulation is the only computational method that can treat DNA origami objects enhanced by non-standard functional groups and characterize the transport phenomena in simulations of DNA origami channels.

All-atom simulations of large-scale DNA origami objects including explicit treatment of water molecules require powerful computational resources. During the past few years, we demonstrated that the Blue Waters supercomputer is ideal for simulations of large-scale DNA origami objects.

Accomplishments

Our work in 2015 has continued computational exploration of exemplary DNA origami systems [22, 23], leading to the publication of two manuscripts [24, 25] and two others submitted for publication [26, 27]. We used our 238,000 node-hour allocation (project JQ5) to perform three large-scale MD simulations of DNA origami systems. First, we characterized the structure and transport properties of prototypical DNA channels. Second, we demonstrated that the MD method can predict DNA origami structure with similar accuracy as costly state-of-the-art high-resolution cryo electron microscopy (cryo-EM) [26]. We also developed a simplified protocol that allows anyone with a desktop computer to perform accurate structure prediction of square-lattice DNA origami objects [26]. Finally, the mechanical and ionic transport properties of an emerging nanotechnology similar to origami—DNA bricks—was investigated. We found that, compared to origami, DNA bricks have a less dense and flexible structure [27].

A1. Bio-mimetic membrane channel of DNA origami.

An important goal of nanotechnology is development of biological and chemical sensors that mimic the functions of membrane protein channels involved in cellular signal transductions. Recently, DNA self-assembly has emerged as a new paradigm for design of the biomimetic membrane channels [2, 11, 28]. Several experimental groups have just demonstrated assembly and insertion of DNA channels into lipid bilayer membranes [11, 28]. Among those biomimetic channels, the 6-helix channel—which consists of six double-stranded DNA

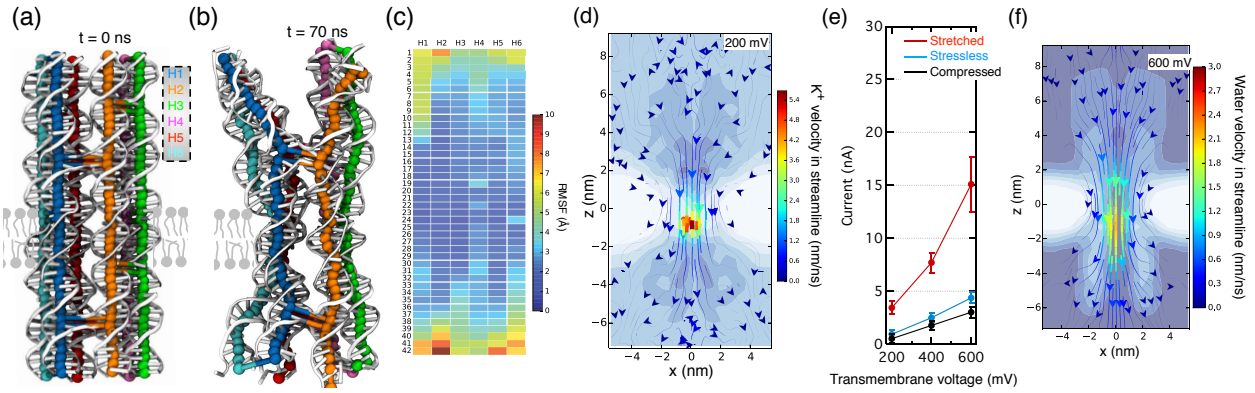

Figure 1: Biomimetic DNA membrane channel. (a) An idealized initial structure shown using a cartoon representation (gray) overlaid with a custom chickenwire representation (colors). In the chickenwire representation, beads indicate the locations of the centers of mass of individual basepairs; horizontal connections between pairs of beads indicate inter-helical crossovers. (b) The channel structure after the 70-ns equilibration in the same representation as panel a. (c) Root-mean-square fluctuations (RMSF) of each base pair's center of mass during the production simulations. (d) Local density (gray scale) and local velocity (streamlines) of K^+ ions at 200 mV. The maps show the xz cross sections of the corresponding three-dimensional (3D) density and velocity fields. (e) The simulated ionic current under compression (black), zero tension (blue), and extension (red) conditions. (f) The average local density (grayscale) and velocity (streamlines) of water during the 400 ns MD simulation at 600 mV.

(dsDNA) helices forming a transmembrane pore of ∼2.5-nm diameter—stands out for its simple design, high yield, and ideal transport properties [28]. To stabilize the 6-helix channel in a lipid bilayer, hydrophobic ethylthiolate groups were chemically added to phosphate groups that lie inside the lipid bilayer, mimicking the hydrophobic belt of protein channels [28]. Despite the successful demonstration of prototypical DNA channels, development of more realistic sensors requires a computational characterization method. Using the Blue Waters supercomputer, we explore the use of atomistic mMD simulations for characterization of DNA channels, characterizing their biophysical properties with atomic precision. The results of our study were published in the *Journal of Physical Chemistry Letters* [25].

Like protein membrane channels, the function of DNA channels depends on their structure. Hence, knowing the structure and mechanical stability of the channel is valuable in selecting a position for active sensing sites. Thus, determining how a realistic structure differs from its idealized design is important. We chose a 6-helix channel, for which ionic conductance is experimentally well-characterized [28]. Our MD simulations showed that, while overall remaining stable, the local structure of the channel undergoes considerable fluctuations, departing from the idealized design, Fig. 1a,b. We also found that the transmembrane domain is structurally stable and compact whereas the periphral domains at each end of the channel are more disordered and undergo relatively larger structural fluctuations, Fig. 1c.

Our MD simulations also revealed the detailed pathway of ionic conductance. The transmembrane ionic current flows both through the central pore of the channel as well as along the DNA walls and through the gaps in the DNA structure, Fig. 1d. At the transmembrane domain, no leakage current was observed at the channel-lipid interface, confirming the stable positioning of the DNA channel in the lipid bilayer, Fig. 1d. Surprisingly, we find the conductance of a DNA channel to depend on the membrane tension, making them potentially suitable for force sensing applications, Fig. 1e. Finally, in our exploratory sim-

ulations of DNA channels for drug delivery applications, we discovered prominent effect of electro-osmotic flow, Fig. 1f, that appear to govern transport of drug-like molecules and can be strong enough to pump charged molecules like ATP agains the transmembrane electrical gradient.

A2. *De novo* DNA origami structure prediction. The cryo-EM method has been used to obtain the most detailed experimental characterization of the *in situ* structure of a DNA origami object called the "pointer" in an effort to describe how DNA origami design deviates from idealized structure [16], Fig. 2A,B. The system used for the study contained 5,238 nucleotides in 82 dsDNA helices and included various types of connections commonly found in DNA origami objects. To test the accuracy of our MD method, we performed a fully atomistic explicit solvent MD simulation of the exact DNA origami design characterized with the cryo-EM method. The caDNAno design provided by Bai *et al.* [16] was converted to an all-atom representation. The simulation ran for ∼200 ns. At the beginning of the simulation, the DNA origami structure quickly departed from its initial idealized configuration of parallel helices toward a conformation characterized by a global right-handed twist, consistent with the cryo-EM reconstruction. The helices, which were tightly packed at the beginning of the simulation, spread into the characteristic chickenwire configuration [22]. The root mean square deviation (RMSD) of the simulated pointer structure from the cryo-EM derived pseudo-atomic model gradually reduced to a value similar to the reported resolution of the cryo-EM reconstruction, Fig. 2C, indicating a very good agreement

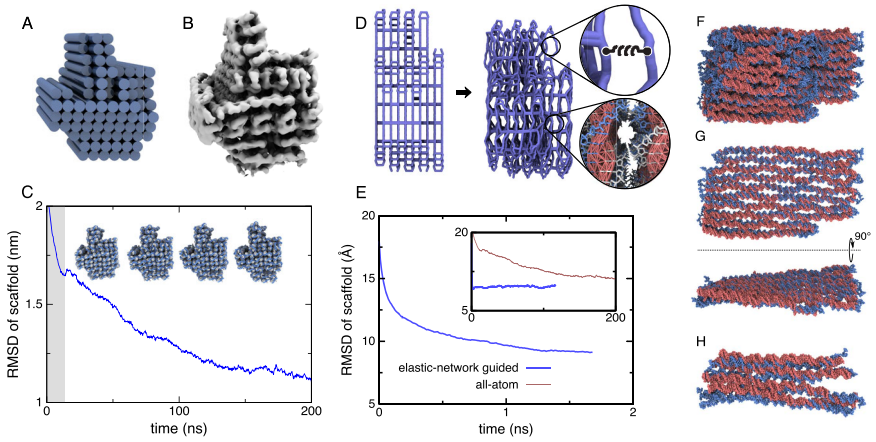

Figure 2: Comparison of all-atom MD simulation of a large DNA origami structure with cryo-EM reconstruction. (A) A three-dimensional (3D) model of the pointer object [16] built according to its idealized design. Each DNA helix is represented by a cylinder. (B) Cryo-electron microscopy reconstruction of the DNA pointer structure [16]. The object's structure is characterized by a 3D electron density map visualized in the figure as a surface of constant electron density. (C) Root mean square displacement (RMSD) of the pointer's coordinates with respect to the model obtained from cryo-EM reconstruction [16] during a 200 ns explicit solvent MD trajectory. The inset depicts the instantaneous conformations of the pointer object during the trajectory. (D) Chickenwire representation of the pointer before (left) and after (right) a 1.7 ns elastic network-guided simulation. Intra-helical elastic network restraints maintaining basepairing and basestacking and while inter-helical restraints maintaining prescribed inter-helical distances are depicted in the lower and upper magnified panels, respectively. (E) RMSD of the pointer during the elastic network-guided simulation. The inset shows the RMSD of the pointer object during explicit solvent simulations with initial coordinates from the end of the elastic network-guided run (blue) and the idealized design (red, same as in panel C). (F-H) Comparison between simulated (blue) and cryo-EM derived (red) structures of the pointer object. (F) The entire pointer object, viewed from the side. (G) A slice of the object showing the characteristic chickenwire pattern. (H) Spreading of the helices due to crossover omission in the design of the pointer structure.

between the simulated and experimentally derived structures. This simulation served as a gold-standard test for the accuracy of our computational model.

The good overall agreement between the simulated and experimentally-derived structures of the pointer object suggests that all-atom MD simulations could be used for testing and prototyping of DNA origami designs. However, explicit solvent simulations of a typical DNA origami object are still too demanding, computationally, to be practical for the routine characterization of DNA origami objects. Hence, we sought an alternative approach that would be less computationally costly but still could provide a reasonably accurate atomistic model. Solvent interactions constitute the majority of the computation during an all-atom simulation, so we eliminated all solvent from our MD model, and also turned long-range electrostatic interactions off to mimic electrostatic screening due to ions. Without solvent, the microscopic structure of a DNA helix breaks down, so we applied an elastic network of restraints to maintain the secondary structure of each DNA helix, Fig. 2D. In addition, harmonic springs were placed between neighboring helices to mimic screened electrostatic repulsion. Amazingly, with this protocol, the pointer structure approached the experimentally-derived configuration ∼100-fold faster than in our explicit solvent all-atom simulation, Fig. 2E. We found that the final configuration obtained from the elastic network-guided simulation agreed well with experiment and was quite stable in subsequent all-atom simulation with explicit solvent, Fig. 2F-H. Our findings are summarized in a manuscript that is currently under review in *Nucleic Acids Research* [26].

A3. Molecular mechanics of DNA bricks.

The DNA brick technique [29] is a DNA origami-like approach that utilizes staggered

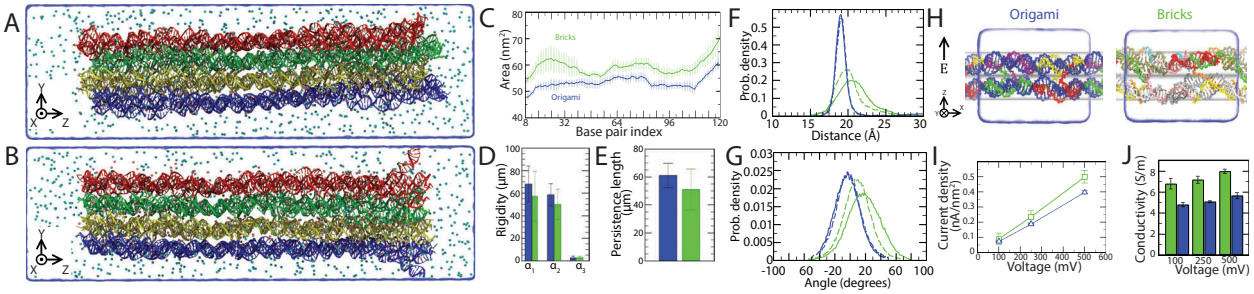

Figure 3: Comparative all-atom MD study of DNA bricks and DNA origami. (A,B) Conformations of DNA origami (A) and DNA brick (B) structures obtained at the end of 165-ns MD simulations. Helices are colored according to their layer in the structure. Ions are shown in green and pink. Water is shown as a semitransparent molecular surface. (C) The local cross-sectional area of the xy plane for the origami (blue) and brick (green) structures versus base pair index. (D,E) Generalized rigidities $\alpha_{1,2,3}$ (D) and persistence lengths (E) of the origami and brick structures. (F,G) Distributions of interhelical distances (F) and dihedral angles (G) at DNA junctions. Blue is origami, solid green is the bonded side of the brick junction, and dashed green is the nonbonded side. Origami and brick junctions generally exhibit left- and right-handed twists, respectively. (H) All-atom model of the origami (left) [24] and brick (right) simulation systems solvated in 1 M KCl and 50 mM $MgCl_2$, with ions removed for clarity. Scaffold strands are represented in blue, with all others being staple strands. The blue semitransparent surface indicates the boundary of the simulation box. The horizontal semitransparent gray cylinders are drawn to distinguish the top and bottom layers There are 4 strands (green, purple, yellow, and red) in origami and 2 strands (pink and orange) in brick connecting to the top and bottom layers in the direction of applied electric field. (I,J) Ionic current density (I) and electrical conductivity (J) versus voltage for origami and brick structures. The brick structure (green) has a higher current density and conductivity than the origami structure (blue) [24] for all voltages tested.

units to build DNA nanostructures with a predefined library, and is similar in appearance to arrays of repeating bricks in a wall. The structures differ from traditional DNA origami in the use of short, 32-nucleotide oligomers with no long scaffold strand, and in a single crossover per connection point compared to a pair of crossovers in DNA origami. These changes increase the yield of self-assembly and make structures easier to design, but may have unknown structural consequences. Hence, we compared the mechanical and ionic conductance properties of DNA brick structures to those of equivalent DNA origami structures.

The DNA brick and square lattice DNA origami systems each contained a ∼44-nm-long bundle of 4096 nucleotides surrounded by an electrolyte with ion concentration matching experiment [29], Fig. 3A,B. The objects were designed so that the structures were equivalent and the sequences identical. The systems were each simulated for 165 ns. The first notable difference between the two was their cross-sectional area, Fig. 3C, which was higher for bricks than for origami. This larger area appears to affect the rigidities, Fig. 3D, and persistence length, Fig. 3E, making brick structures marginally weaker overall. The higher area arises from a wider spacing between adjacent helices in DNA bricks, see Fig. 3F, which is in turn caused by the fewer number of crossovers per junction for DNA bricks. Figure 3G demonstrates that the brick junctions exhibit a right-handed twist on average, while origami junctions adopt a left-handed twist.

A smaller simulation system was used to compare the ionic conductivity of DNA brick to the conductivity previously determined for an equivalent DNA origami structure [24], Fig. 3H. The system was equilibrated for ∼400 ns, and the structure with the greatest similarity in terms of xy cross-sectional area to the origami structure was used to initialize production simulations. Three different biases (100, 250, and 500 mV) were applied to the systems for 48 ns. Our study of DNA origami indicated that the conductivity is reduced when the DNA density is increased [24]. Hence, the wider inter-helical spacing of DNA bricks suggests that brick structures would have a higher conductivity, which was corroborated by the ionic current density, Fig. 3I, and conductivity Fig. 3J.

In summary, we found that the lower number of crossovers in DNA bricks result in less dense and less rigid structures that conduct ions more readily than DNA origami. A manuscript describing these findings has been submitted for publications [27].

List of publications and presentations associated with this work

- S. Banerjee, J. Wilson, J. Shim, M. Shankla, E. A. Corbin, A. Aksimentiev, and R. Bashir. Slowing DNA transport using graphene–DNA interactions. *Advanced Functional Materials*, 25:936–946, 2015.

- C.-Y. Li, E. A. Hemmig, J. Kong, J. Yoo, S. Hernández-Ainsa, U. F. Keyser, and A. Aksimentiev. Ionic conductivity, structural deformation and programmable anistropy of DNA origami in electric field. *ACS Nano*, 9:1420–1433, 2015.

- J. Yoo and A. Aksimentiev. Molecular dynamics of membrane-spanning DNA channels: Conductance mechanism, electro-osmotic transport and mechanical gating. *Journal*

of Physical Chemistry Letters, 6:4680–4687, 2015.

- M. Belkin, S.-H. Chao, M. P. Jonsson, C. Dekker, and A. Aksimentiev. Plasmonic nanopores for trapping, controlling displacement, and sequencing of DNA. *ACS Nano*, 9:10598–10611, 2015.

- Y. X. Shen, W. Si, M. Erbakan, K. Decker, R. D. Zorzi, P. O. Saboe, Y. J. Kang, S. Majd, P. J. Butler, T. Walz, A. Aksimentiev, J. li Hou, and M. Kumar. Highly permeable artificial water channels that self-assemble into two-dimensional arrays. *Proceedings of the National Academy of Sciences, USA*, 112:9810–9815, 2015.

- C. Maffeo, J. Yoo, and A. Aksimentiev. *De novo* prediction of DNA origami structures through atomistic molecular dynamics simulation. Under review at *Nucleic Acids Research*.

- S. Slone, J. Yoo, C.-Y. Li, and A. Aksimentiev. Molecular mechanics of DNA bricks: *In situ* structure, mechanical properties and ionic conductivity. Submitted.

- M. Belkin and A. Aksimentiev. Molecular dynamics simulation of DNA capture and transport in heated nanopores. Submitted.

- (Presentation) A. Aksimentiev. Molecular dynamics of DNA origami. NCSA Blue Waters Symposium for Petascale Science and Beyond. Sunriver, Oregon. May 2015.

- (Presentation) A. Aksimentiev. DNA Ion Channels Telluride Science Workshop on Ion Channel Biophysics. Telluride, Collorado. July 2015

- (Presentation) A. Aksimentiev. Nanopore Sequencing: State of the Art and Future Directions. 5th Annual Next Generation Sequencing Asia Congress Singapore, October 2015.

- (Presentation) A. Aksimentiev. Surprising Physics of DNA. Department of Physics, Colloquium. Michigan Institute of Technology. November 2015.

- (Presentation) C.-Y. Li Ionic Conductivity, Structural Deformation, and Programmable Anisotropy of DNA Origami in Electric Field. FNANO2015. Snowbird, Utah. April 2015.

- (Presentation) C.-Y. Li Ionic Conductivity, Structural Deformation, and Programmable Anisotropy of DNA Origami in Electric Field. Student–Postdoc Biophysics Symposium. Urbana, IL, May 2015.

- (Poster) C. Maffeo, J. Yoo, and A. Aksimentiev. *De novo* prediction of DNA origami structure through atomistic molecular dynamics simulation. DNA21: 21st International Conference on DNA Computing and Molecular Programming. Wyss Institute for Biologically Inspired Engineering, Harvard University, Boston, MA. August 17-21, 2015.

Plan for the next year

We have planed three individual projects involving DNA origami for the next year. The first (P1) is the continuation of the project summarized in Accomplishment A1. The other two (P2, and P3) involve new simulations of DNA origami objects. In Project P2, we will reveal the molecular mechanism driving the self-assembly of so-called "shape-complementary" DNA origami structures, which can be used to construct higher-order nanostructures that feature ion concentration-dependent assembly. Finally, using structures obtained in project P2 as target data, we will extend our elastic network-guided simulation protocol of the square lattice DNA origami to the honeycomb lattice (P3). Using the latest version of the NAMD package [30, 31], we have found that we need to use 80 node hours to perform a 1-ns (NS) simulation of a 1-million-atom (MA) system, or 80 NH/MANS. We used this factor to estimate the requested allocation for each project. Projects P1, P2, and P3 will require 83,000, 133,000, and 24,000 node hours, respectively, resulting in the **total requested allocation of 240,000 node hours**. P1 will be performed during Q1, P2 during Q1 and Q2, and P3 will be performed during Q2 and Q3.

P1. Ionic conductance of the scalable DNA channels. Membrane protein channels involved in cellular signal transductions are fascinating biological sensors with high selectivity and efficiency. Recently, it was demonstrated that DNA origami-based channels can mimic the ionic conductance and transport properties of membrane protein channels [11, 28, 32, 33, 34, 35]. A typical DNA channel is made by arranging a few parallel DNA double helices as a polygon. The central cavity of the polygon is the transmembrane pore. The inner diameter of the DNA channel depends on the arrangement and the number of DNA double helices. To stabilize the DNA channels in a lipid bilayer membrane, the DNA channel has to be "anchored" to the lipid bilayer membrane with different hydrophobic groups, such as ethylthiolate [28], cholesterol [11, 34, 35] or porphyrin [32, 33], which are covalently connected to the channel. Until now, most of the DNA channel designs arrange 4 or 6 parallel DNA double helices as a square [34] or hexagon [28, 32, 33, 35], giving an inner channel diameter of 1-2.5 nm. To the best of our knowledge, all published DNA origami channels have 6 or fewer helices in the transmembrane region, even the largest channel made with 54 DNA double helices [11]. Although the designs and functions of the self-assembled DNA structures have skyrocketed over the past decade [3, 6, 14, 29], the design space of the DNA channels is still poorly explored.

The most common experimental characterization of a DNA channel embedded in a lipid bilayer membrane is the single-molecule current measurement. In collaboration with the Keyser group from University of Cambridge, we aim to systematically investigate how the conductance of a DNA channel scales with its size. Based on the designs from the Keyser group and the Howorka group [35], we have built a range of simulation models for DNA channels made from 1 helix to 112 helices, Fig. 4. Hydrophobic groups are attached around the DNA channels to stabilize the channel-lipid assembly. We have performed preliminary simulations to equilibrate the DNA channel structures and the channel-lipid interface. Next, we will simulate the DNA channel systems under an electric field to determine the ionic current through the channels. In order to directly compare our simulation results with experiment [34], we will simulate all channels under -100 mV, -30 mV, 30 mV and 100 mV transmembrane voltages. Based on our past experience with the 6-helix channel simula-

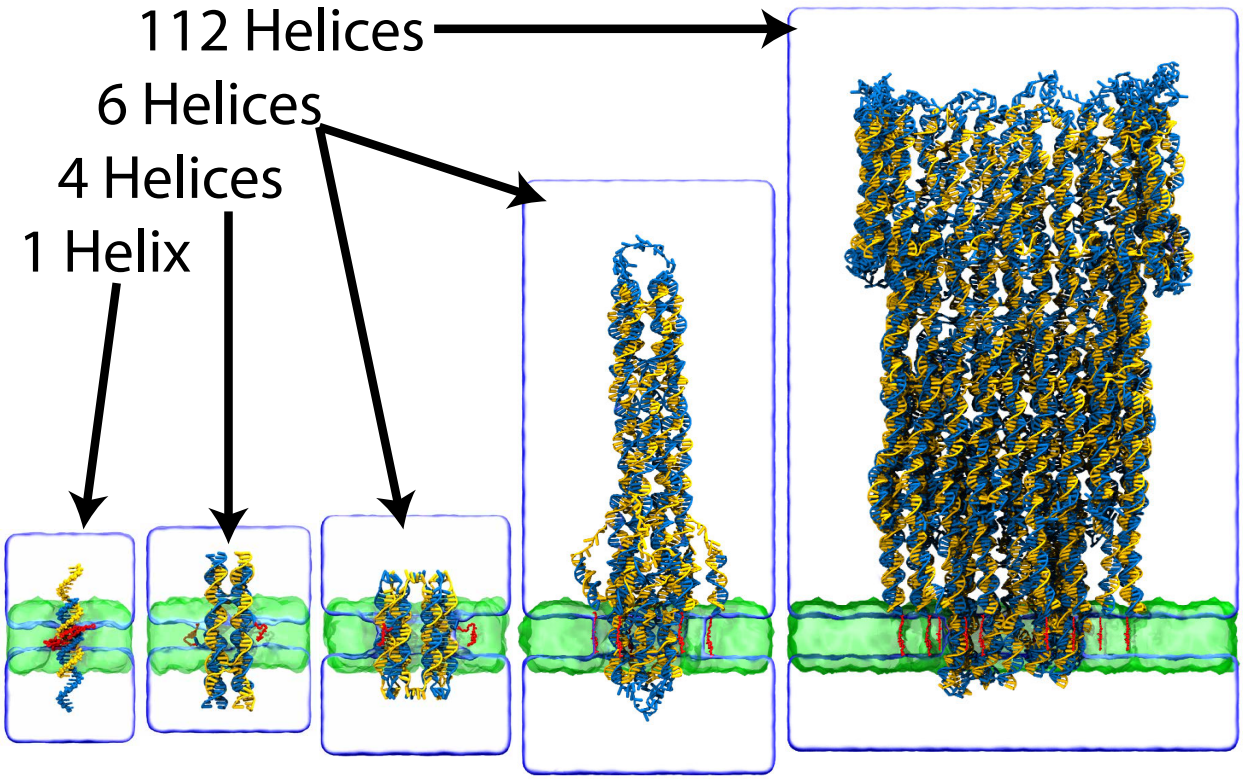

Figure 4: Schematics of a range of DNA channels (blue and yellow) made with different numbers of DNA double helices. The DNA channels are inserted in the lipid bilayer membrane (green semitransparent surface) with the help of hydrophobic groups (red). From left to right, the number of atoms in each simulation cell (blue semitransparent surface) are: 1.4×10^5 atoms (1 helix), 2.4×10^5 atoms (4 helices), 3.1×10^5 atoms (6 short helices, designed by Burns *et al.* [35]), 1.8×10^6 atoms (6 long helices) and 8.0×10^6 atoms (112 helices).

tion [25], we plan to simulate the 112-helix channel (8.0×10^6 atoms) for 8 ns, the six-long helix channel (1.8×10^6 atoms) for 30 ns, the six-short helix channel (3.1×10^5 atoms) for 150 ns, the four-helix channel (2.4×10^5 atoms) for 200 ns, and the one-helix channel (1.4×10^5 atoms) for 340 ns at each transmembrane bias. The simulation time needed to obtain statistically significant measure of the ionic current increases as the channels become smaller because their conductance is expected to decrease with their size, requiring longer simulations times to observe the same number of ion permeation events. Summing up those numbers, the total computational resources needed for one bias is 260.1 MANS. Therefore, this project will require 80 NH/MANS $\times$ 4 biases $\times$ 260.1 MANS = 83,000 node hours.

P2. Complementary shaped DNA origami assembly.

Engineering a custom DNA nanostructure used to be restricted to a single scaffold. Recently, Gerling *et al.* [14] extended the DNA origami technique by developing multiple DNA components with complementary shapes that spontaneously assemble together without base pairing, Fig. 5. Experimentally, Gerling *et al.* demonstrated that increasing the surrounding cationic concentration, and decreasing the temperature, increases the probability that these multi-domain DNA structures overcome the electrostatic repulsion and assemble together into a closed conformation [14]. Stacking bonds are known to be important for stabilizing these assemblies, but the underlying physical mechanism by which these complementary-

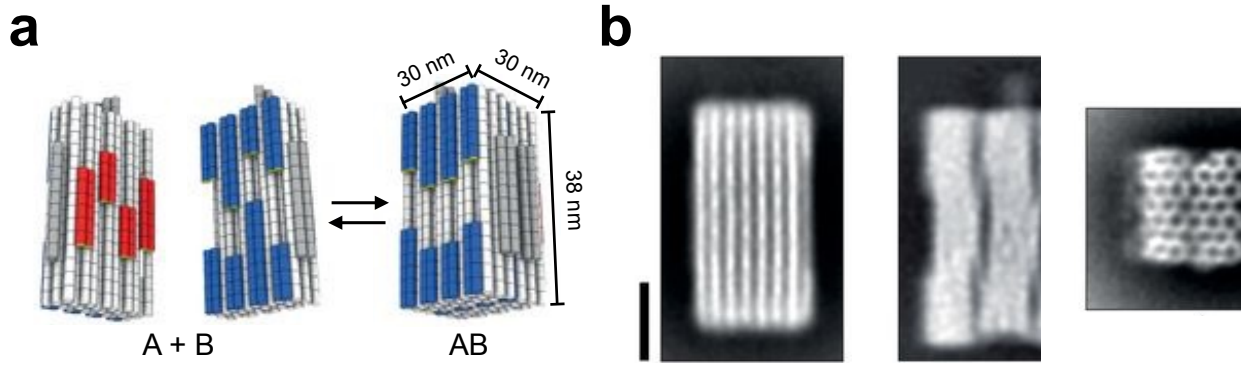

Figure 5: Shape-based assembly of DNA objects. (a) A schematic representation of two complementary-shaped DNA origami components. Colors highlight double-helical DNA protrusions (red) and recessions (blue). (b) Average negative-strain TEM micrographs of the self-assembled DNA dimeric object AB in 25 mM $MgCl_2$. Scale bar, 20 nm. This figure is adapted from Ref. 14.

shaped DNA components fit together requires further explanation.

We will investigate the effects of cationic concentration and temperature on two complementary-shaped DNA nanostructures, Fig. 5a, using all-atom MD simulations in explicit solvent, examining the deformations and overall flexibility of the designed interface under the following conditions: (i) 5 mM NaCl + 5 mM $MgCl_2$ at 298 K; (ii) 5 mM NaCl + 25 mM $MgCl_2$ at 298 K; (iii) 5 mM NaCl + 25 mM $MgCl_2$ at 323 K; and (iv) 5 mM NaCl + 50 mM $MgCl_2$ at 298 K. Each of the two DNA domains with complementary shapes, 'A' and 'B' in Fig. 5a, will be placed in a $19 \times 34 \times 40$ nm^3 solvated box containing ∼2,600,000 atoms. Based on the convergence timescale of our previous simulation [26], we will perform ∼80 ns production MD simulations. By analyzing structural fluctuations of the complementary-shaped DNA components and their dependence on the ionic strength and temperature, we expect to learn about the microscopic mechanism underlying the shape-based assembly. This project will require 80 NH/MANS × (2 × 2.6) million atoms × 80 ns × 4 conditions = 133,000 node hours.

P3. Structure prediction protocol for honeycomb lattice DNA origami. While investigating the DNA origami structure with a known structure determined by cryo-EM, we discovered that it is possible to obtain a high-quality structure from vacuum simulations guided by an intrahelical elastic network of restraints and a set of interhelix restraints [26]. When we attempted to employ the elastic network-guided simulation protocol to DNA origami objects with honeycomb lattice, we were surprised that the protocol failed to produce structures consistent with transmission electron microscope images [5]. Specifically, structures with a programmed bend became unexpectedly twisted in our simulations, see Fig. 6a,b. We next verified that the twist occurs for a simple six-helix bundle, see Fig. 6c-e. We then began varying the elastic network parameters in an effort to remove the twist, but in roughly a dozen simulations we were unable to accomplish that.

Here we propose an ensemble of simulations that will explore the parameter space to determine the optimal protocol for honeycomb lattice DNA origami simulations. The parameter space that we will explore includes the following: (a) spring constants of the intrahelical elastic network restraints (3 values: 0.01, 0.1, 1 kcal/mol $Å^2$), (b) spring constants of the interhelical chickenwire restraints (3 values: 0.01, 0.1, 1 kcal/mol $Å^2$), (c) rest length

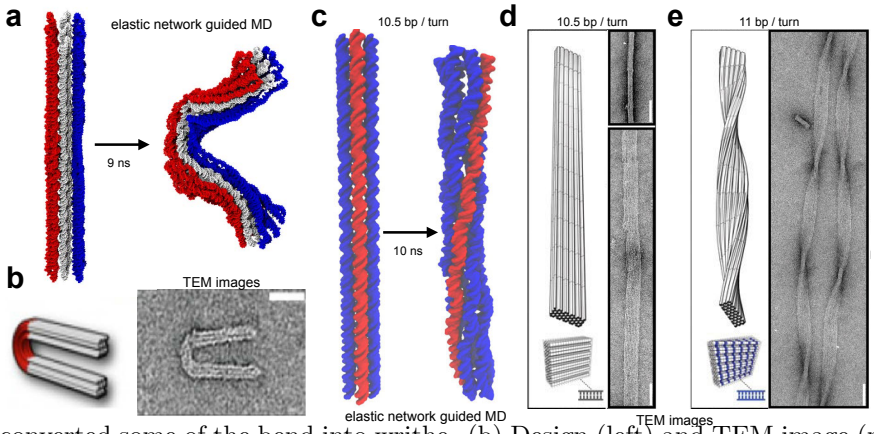

Figure 6: Comparison of honeycomb lattice structures obtained using the elastic network simulation protocol and observed through transmission electron microscopy (TEM). (a) A honeycomb lattice DNA origami object designed to have a 180° bend before (left) and after (right) an elastic network-guided simulation. A right-handed twist that developed during the simulation converted some of the bend into writhe. (b) Design (left) and TEM image (right) of the DNA origami object with a 180° bend. The TEM image does not appear to depict a twisted structure. (c) A simple six-helix DNA origami bundle before (left) and after (right) an elastic network-guided simulation. The structure develops a significant right-handed twist. (d,e) TEM images of similar DNA origami objects. By controlling the density of crossovers, objects can be created with a normal (d) or high (e) number basepairs per turn that are untwisted and twisted, respectively. Panels b, d, and e are adapted from Ref. 5.

of the interhelical restraints (5 values: 28, 29, 30, 31, 32 Å), (d) number and placement of the interhelical chickenwire restraints (3 values: 7, 5, 3 bonds), and (e) dielectric constant of short-range coulomb interactions (2 values: 1, 80). We will run a simulation for each combination of parameters for about 2 ns, and quantify the twist and the RMSD with respect to the target structure. Because no honeycomb lattice DNA origami structure has been determined experimentally with high resolution, we will use one of the block structures obtained from the preceding project as target data. With no solvent molecules included explicitly, each system will contain ∼560,000 atoms. Hence this project will require 80 NH/MANS × 0.56 million atoms × 2 ns × (3 × 3 × 5 × 3 × 2) conditions = 24,000 node hours.

References

[1] N. C. Seeman. Nanomaterials based on DNA. *Annual Review of Biochemistry*, 79:65–87, 2010.

[2] A. V. Pinheiro, D. Han, W. M. Shih, and H. Yan. Challenges and opportunities for structural DNA nanotechnology. *Nature Nanotechnology*, 6:763–72, 2011.

[3] P. W. K. Rothemund. Folding DNA to create nanoscale shapes and patterns. *Nature*, 440:297–302, 2006.

[4] S. M. Douglas, H. Dietz, T. Liedl, B. Högberg, F. Graf, and W. M. Shih. Self-assembly of DNA into nanoscale three-dimensional shapes. *Nature*, 459:414–8, 2009.

[5] H. Dietz, S. M. Douglas, and W. M. Shih. Folding DNA into twisted and curved nanoscale shapes. *Science*, 325:725–30, 2009.

[6] D. Han, S. Pal, J. Nangreave, Z. Deng, Y. Liu, and H. Yan. DNA origami with complex curvatures in three-dimensional space. *Science*, 332:342–6, 2011.

[7] E. S. Andersen, M. Dong, M. M. Nielsen, K. Jahn, R. Subramani, W. Mamdouh, M. M. Golas, B. Sander, H. Stark, C. L. P. Oliveira, J. S. Pedersen, V. Birkedal, F. Besenbacher, K. V. Gothelf, and J. Kjems. Self-assembly of a nanoscale DNA box with a controllable lid. *Nature*, 459:73–6, 2009.

[8] T. Liedl, B. Högberg, J. Tytell, D. E. Ingber, and W. M. Shih. Self-assembly of three-dimensional prestressed tensegrity structures from DNA. *Nature Nanotechnology*, 5:520–4, 2010.

[9] C. Lin, R. Jungmann, A. M. Leifer, C. Li, D. Levner, G. M. Church, W. M. Shih, and P. Yin. Submicrometre geometrically encoded fluorescent barcodes self-assembled from DNA. *Nature Chemistry*, 4:832–839, 2012.

[10] J.-P. J. Sobczak, T. G. Martin, T. Gerling, and H. Dietz. Rapid folding of DNA into nanoscale shapes at constant temperature. *Science*, 338:1458–61, 2012.

[11] M. Langecker, V. Arnaut, T. G. Martin, J. List, S. Renner, M. Mayer, H. Dietz, and F. C. Simmel. Synthetic lipid membrane channels formed by designed DNA nanostructures. *Science*, 338:932–6, 2012.

[12] G. P. Acuna, F. M. Möller, P. Holzmeister, S. Beater, B. Lalkens, and P. Tinnefeld. Fluorescence enhancement at docking sites of DNA-directed self-assembled nanoantennas. *Science*, 338:506–10, 2012.

[13] A. Kuzyk, R. Schreiber, Z. Fan, G. Pardatscher, E.-M. M. Roller, A. Högele, F. C. Simmel, A. O. Govorov, and T. Liedl. DNA-based self-assembly of chiral plasmonic nanostructures with tailored optical response. *Nature*, 483:311–4, 2012.

[14] T. Gerling, K. F. Wagenbauer, A. M. Neuner, and H. Dietz. Dynamic DNA devices and assemblies formed by shape-complementary, nonbase pairing 3D components. *Science*, 347:1446–1452, 2015.

[15] D. J. Kauert, T. Kurth, T. Liedl, and R. Seidel. Direct mechanical measurements reveal the material properties of three-dimensional DNA origami. *Nano Letters*, 11:5558–5563, 2011.

[16] X.-C. C. Bai, T. G. Martin, S. H. W. Scheres, and H. Dietz. Cryo-EM structure of a 3D DNA-origami object. *Proceedings of the National Academy of Sciences, USA*, 109:20012–7, 2012.

[17] D.-N. Kim, F. Kilchherr, H. Dietz, and M. Bathe. Quantitative prediction of 3D solution shape and flexibility of nucleic acid nanostructures. *Nucleic Acids Research*, 2011.

[18] K. Pan, D.-N. N. Kim, F. Zhang, M. R. Adendorff, H. Yan, and M. Bathe. Lattice-free prediction of three-dimensional structure of programmed DNA assemblies. *Nature Communications*, 5:5578, 2014.

[19] T. E. Ouldridge, A. A. Louis, and J. P. K. Doye. Structural, mechanical, and thermodynamic properties of a coarse-grained DNA model. *The Journal of Chemical Physics*, 134:085101, 2011.

[20] T. E. Ouldridge, R. L. Hoare, A. A. Louis, J. P. K. Doye, J. Bath, and A. J. Turberfield. Optimizing DNA nanotechnology through coarse-grained modeling: a two-footed DNA walker. *ACS Nano*, 7:2479–90, 2013.

[21] C. Maffeo, T. T. M. Ngo, T. Ha, and A. Aksimentiev. A coarse-grained model of unstructured single-stranded DNA derived from atomistic simulation and single-molecule experiment. *Journal of Chemical Theory and Computation*, 10:2891–2896, 2014.

[22] J. Yoo and A. Aksimentiev. In situ structure and dynamics of DNA origami determined through molecular dynamics simulations. *Proceedings of the National Academy of Sciences, USA*, 110:20099–20104, 2013.

[23] J. Yoo, A. N. Sobh, C.-Y. Li, and A. Aksimentiev. Cadnano to PDB file converter.

[24] C.-Y. Li, E. A. Hemmig, J. Kong, J. Yoo, S. Hernández-Ainsa, U. F. Keyser, and A. Aksimentiev. Ionic conductivity, structural deformation and programmable anistropy of DNA origami in electric field. *ACS Nano*, 9:1420–1433, 2015.

[25] J. Yoo and A. Aksimentiev. Molecular dynamics of membrane-spanning DNA channels: Conductance mechanism, electro-osmotic transport and mechanical gating. *Journal of Physical Chemistry Letters*, 6:4680–4687, 2015.

[26] C. Maffeo, J. Yoo, and A. Aksimentiev. *De novo* prediction of DNA origami structures through atomistic molecular dynamics simulation. Under review at *Nucleic Acids Research*.

[27] S. Slone, J. Yoo, C.-Y. Li, and A. Aksimentiev. Molecular mechanics of DNA bricks: *In situ* structure, mechanical properties and ionic conductivity. Submitted.

[28] J. R. Burns, E. Stulz, and S. Howorka. Self-assembled DNA nanopores that span lipid bilayers. *Nano Letters*, 13:2351–2356, 2013.

[29] Y. Ke, L. L. Ong, W. M. Shih, and P. Yin. Three-dimensional structures self-assembled from DNA bricks. *Science*, 338:1177–1183, 2012.

[30] L. Kalé, R. Skeel, M. Bhandarkar, R. Brunner, A. Gursoy, N. Krawetz, J. Phillips, A. Shinozaki, K. Varadarajan, and K. Schulten. NAMD2: Greater scalability for parallel molecular dynamics. *Journal of Computational Physics*, 151:283–312, 1999.

[31] J. C. Phillips, R. Braun, W. Wang, J. Gumbart, E. Tajkhorshid, E. Villa, C. Chipot, R. D. Skeel, L. Kale, and K. Schulten. Scalable molecular dynamics with NAMD. *Journal of Computational Chemistry*, 26:1781–1802, 2005.

[32] J. R. Burns, K. Göpfrich, J. W. Wood, V. V. Thacker, E. Stulz, U. F. Keyser, and S. Howorka. Lipid-bilayer-spanning DNA nanopores with a bifunctional porphyrin anchor. *Angewandte Chemie International Edition*, 52:12069–12072, 2013.

[33] A. Seifert, K. Göpfrich, J. R. Burns, N. Fertig, U. F. Keyser, and S. Howorka. Bilayer-spanning DNA nanopores with voltage-switching between open and closed state. *ACS Nano*, 9:1117–26, 2015.

[34] K. Göpfrich, T. Zettl, A. E. C. Meijering, S. Hernández-Ainsa, S. Kocabey, T. Liedl, and U. F. Keyser. DNA-tile structures induce ionic currents through lipid membranes. *Nano Letters*, 15:3134–3138, 2015.

[35] J. R. Burns, A. Seifert, N. Fertig, and S. Howorka. A biomimetic DNA-based channel for the ligand-controlled transport of charged molecular cargo across a biological membrane. *Nature Nanotechnology*, 2016.